Supplementary Information for

Depression-like Episodes in Mice Harboring mtDNA Deletions in Paraventricular Thalamus

Takaoki Kasahara, Atsushi Takata, Tomoaki M. Kato,
Mie Kubota-Sakashita, Tomoyo Sawada, Akiyoshi Kakita, Hiroaki Mizukami,
Daita Kaneda, Keiya Ozawa, and Tadafumi Kato

The PDF file includes:

SUPPLEMENTARY MATERIALS AND METHODS

Animals

All mutant *Polg*1 transgenic mice used were heterozygotes. Male mutant mice were used for mating with C57BL/6JJcl female mice (CLEA Japan, Tokyo, Japan); the mouse strain was originally used for the generation of the transgenic mice. Genomic DNA was isolated from tail biopsies, and the genotyping was performed by multiplex PCR using the two sets of primers: Fw, 5′-TGG TGA AAC AGT TGA ATC TTC C-3′; Rv, 5′-GTC AGG AGA TTG GTG ATC TGC-3′; and Fw, 5′-AGT GAG TTG AAA GCC ATG GTG-3′; Rv, 5′-GTG GTT GAA CTG CAT CAG TAG G-3′. Controls were non-Tg littermates whenever possible. The mice were kept in a regulated room environment (22.8–23.8 °C, 50 ± 5% humidity). We initially generated three *Polg1* mutant mice lines and selected one line (C57BL/6J-Tg(Camk2-mutPolg)1Bsi),[18] which has been deposited in RIKEN BioResource Center (RBRC01498). *CaMKII*α-promoter-loxP-STOP-loxP-tTA (Tg2) and *TetO*-TeTX (Tg3) transgenic mice were generated as described previously.[19] For AAV-induced region-specific inhibition of neural transmission, heterozygous Tg2 and Tg3 were crossed to obtain the mice (Tg2/+;Tg3/+) which express TeTX depending on Cre recombinase expression and the other progenies (single mutant of Tg2/+ or Tg3/+, or wild-type +/+) were used as control mice. In behavioral analysis, animals were excluded when they were injured or died due to an accident.

Long-term recording of wheel-running activity

Recoding and analyses of wheel-running activity were performed as described previously.[18] Mice were individually housed in cages (24 cm wide × 11 cm deep × 14 cm high) equipped with a running wheel (5 cm wide × 14 cm in diameter). LD 12:12 h cycles (lights on at 8:00 local time) were controlled by a PC computer system (O'Hara & Co., Tokyo, Japan). Light was provided by white LED and the intensity was 20–50 lux at the level of mouse's eyes in the cage. Food and water were available *ad libitum* at all times unless otherwise specified. Wheel-running activity was recorded by an online PC computer system (O'Hara & Co.). Approximately 10–15% of female *Polg1* mutant mice did not acquire running on a wheel or showed less activity (daily wheel rotations < 5,000). Any data obtained from such animals were excluded. The light period activity (%) is defined as a percent of the activity during the light period (12 h; 8:00–20:00 local time; zeitgeber time [ZT] 0–12) divided by the total activity during the whole day (24 h; 8:00–8:00 the next day; ZT 0–24).

Definition of the episodic hypoactivity

We applied the Relative Strength Index (RSI) for the criteria for determining the prolonged

hypoactivity.[35] The RSI compares magnitude of recent gains in a given time period (average up move; U) with magnitude of losses in that period (average down move; D) as follows:

$$\mathrm{RSI} = 100 \times \frac{U}{U + D}$$

We used a 9-day period, which unfailingly covered two estrous cycles of mice. The operational criteria for the prolonged hypoactivity are (1) RSI should be less than 25 at least for one day, and (2) RSI should be less than 50 for consecutive 9 days or more (Supplementary Figure 1a). The first day when RSI declined to less than 50 is defined as the onset of the episode. The termination of the episode is determined by "reverse RSI", which is equivalent to

$$\mathrm{Reverse\ RSI} = 100 \times \frac{D'}{U' + D'}$$

where U' is the average up move in the subsequent 9 days and D' is the average down move in that period.

Ovariectomy

Female *Polg1* mutant mice at 24–36 weeks of age were either sham-operated or ovariectomized under isoflurane anesthesia. Before surgery, these mice were housed in cages with access to a wheel for five weeks. Animals were allowed about two weeks to recover from surgery in cages without a wheel, and then they were housed in cages with a running wheel for about five months.

Long-term escitalopram treatment

Escitalopram oxalate was kindly provided by Lundbeck (Valby, Denmark). In a preliminary experiment, we added escitalopram oxalate at various concentrations (0, 75, 150, 225 μg/mL escitalopram base) and gave them to female mice (C57BL/6J) for 10 days to see the effect of escitalopram on immobility time in forced swimming and tail suspension tests as described above. Immobility time of mice treated with 150 or 225 μg/mL significantly decreased in the forced swimming test. In the tail suspension test, immobility time of mice decreased in a dose-dependent manner, but not significantly. After the behavioral despair tests, plasma was collected and escitalopram level was measured using liquid chromatography-tandem mass spectrometer (Toray Research Center, Inc., Kamakura, Japan). Plasma levels of mice treated with 75, 150, or 225 μg/mL were 2.0 ± 0.7, 88.5 ± 15.1, 94.5 ± 48.4 ng/mL (mean ± SD), respectively. Although the therapeutic level in humans has not been established, plasma level of treated patients was 20–80 ng/mL. These preliminary results showed that drinking water containing 150 μg/mL escitalopram

base was the best treatment method. To see the effect of escitalopram on the episodic hypoactivity, we administered female *Polg1* mutant mice with the escitalopram-containing drinking water in a cross-over design. After an initial 12 week baseline measurement, the *Polg1* mutant mice were randomly divided into two age-matched, episode frequency-matched groups (A and B). Mice in Group A ($n = 12$) were treated with escitalopram for 12 weeks (Period 1) followed by without escitalopram for 12 weeks (Period 2). Mice in Group B ($n = 11$) were given water in Period 1 and escitalopram-containing water in Period 2. The transition period was excluded from the analysis.

Long-term lithium treatment

Giving lithium to mice and to maintain the therapeutic plasma level shown in humans (0.6–1.2 mM Li^+) for months and longer is quite difficult maybe due to difference in renal function. Plasma level of Li^+ reached to the therapeutic level, when C57BL/6 mice fed Li_2CO_3-containing chow diet ($\geq$ 2.4 g/kg).[18] However, mice became polyuria within approximately three weeks after treatment. To treat mice with lithium over long periods, we tested several conditions and found that LiCl 1.7 g/kg diet with a salt solution (450 mM NaCl) as well as water[20] was the best choice for long-term lithium treatment avoiding diabetes insipidus. To see the effect of lithium on the episodic hypoactivity, we administered female Tg mice with LiCl-containing diet (1.7 g/kg) (Oriental Yeast Co., Tokyo, Japan) in a cross-over design. After an initial 12 week baseline measurement, the *Polg1* mutant mice were randomly divided into two age-matched, episode frequency-matched groups (A and B). Mice in Group A ($n = 15$) were treated with lithium for 12 weeks (Period 1) followed by without lithium diet for 12 weeks (Period 2). Mice in Group B ($n = 15$) were given a normal diet in Period 1 and a lithium-containing diet in Period 2. Treated mice were given bottles, one with 450 mM NaCl solution and another with water. The plasma level of Li^+ after 12 weeks of the treatment, measured by atomic absorption spectroscopy (SRL, Inc., Tachikawa, Japan), was 0.17 $\pm$ 0.05 mM (mean $\pm$ SD). All of the treated mice looked healthy, but half of them drunk water more than 10 times as much as untreated mice after 12 weeks of the administration.

Quantification of fecal corticosterone

Feces from mice, which were kept in individual cages with a wheel, were collected once or twice a week for more than four months. To facilitate collecting feces, we used strip-type beddings (Pulsoft, Oriental Yeast Co.; Pulmas μ, Material Research Center Co., Kawasaki, Japan). The collected feces were stored at −20 °C or −80 °C until analysis. Fecal samples were completely dried, weighted, and thoroughly grinded. Corticosterone was extracted

essentially according to the method described by Touma *et al.*[36] One milliliter of aqueous ethanol [ethanol:deionized distilled water (DDW), 8:2 (v/v)] was added to 50 mg of fecal powder, boiled (99 °C) for 5 min, and vortexed for 10 min. The boiling and vortexing steps were repeated additionally twice. After centrifugation (10 min at 2,500 × *g*), the supernatant was poured into another tube and stored at −20 °C until ELISA assay. We used the Corticosterone Enzyme Immunoassay Kit (Arbor Assays, Ann Arbor, MI, USA), according to the manufacturer's protocol. An aliquot of 2.5 µL of the supernatant was added to one well of the ELISA plate.

Long-term EEG/EMG recording and sleep analysis

Female *Polg1* mutant mice (~20 weeks old) were housed in cages with running wheels for one month prior to surgical implantation of telemetry transmitters (F20-EET; Data Sciences International, St. Paul, MN, USA) for recording of EEG, EMG, and locomotor activity. Under isoflurane anesthesia, two EEG electrodes were contralaterally placed into the skull, 1 mm anterior to bregma and 1 mm lateral to the sagittal suture, leaving the dura mater intact. Two EMG electrodes were sutured into the neck musculature. Animals were allowed at least two weeks to recover from surgery in cages without a wheel, and then they were housed in cages with a running wheel for about six months. Because the battery life of the telemetry transmitter was six weeks according to the manufacture's specifications, we switched off the transmitter during euthymic condition of each mouse. We switched on the transmitter and started polysomnographic recordings, when we detected a sign of occurrence of the hypoactivity episode. The EEG and EMG signals were recorded with a sampling rate of 100 Hz, transferred to a receiver placed under the cage, and acquired by Dataquest A.R.T. hardware and software (Data Sciences International). We switched off the transmitter 1–2 weeks after the termination of the hypoactivity episode. The EEG and EMG signals were digitally filtered (EEG, 0.5–30 Hz; EMG, 20–50 Hz), and then data in 10-sec epochs were classified as either wake (high-amplitude EMG and mixed-frequency, low-amplitude EEG), NREM sleep (low-frequency, high-amplitude EEG, low-amplitude EMG, and no locomotion), or REM sleep (theta-dominated EEG, EMG atonia, and no locomotion) with the aid of a sleep scoring software (Sleep Sign; Kissei Comtec, Matsumoto, Japan). Cumulative time spent in NREM and REM (total sleep time) in 24 h or in the light period (ZT 0–12) was calculated. Average total sleep time after hypoactivity episode (euthymic state) was calculated using the data from the same number of days as the number of polysomnographically-recorded days of the episode. The data of the days of change of cages were omitted from the calculations.

Monitoring body temperature and ambulatory activity

Core body temperature (T_b) was continuously monitored using a telemetry system (Data Sciences International). Mice were anesthetized with avertin, and a radiotelemetry transmitter (TA-F20) was implanted intra-abdominally. Two weeks after the operation, the mice were housed in cages with a wheel, and wheel-running activity and T_b were simultaneously measured for half a year. T_b values (10 s average) were collected every 10 min. Ambulatory activity was calculated based on the fluctuation during the 10-s bin in signal intensity of the radio waves emitted from a telemetry probe.

Behavioral test battery during hypoactivity episode

Forty-three female *Polg1* mutant mice (29 Tg, 14 non-Tg) were used in this behavioral analysis. We recorded the wheel-running activity for 30 weeks as described above and conducted a behavioral test battery when an animal exhibited episodic hypoactivity. On the same days, a Tg littermate in euthymic state and a non-Tg littermate in euthymic state were also tested as controls. If littermates were not available, we tested other mice of similar ages. On the first day of the test battery, open field test (12:00–13:00 local time), Y-maze test (13:00–14:00), and forced swimming test (16:00–17:00) were performed. Mice were returned to home cages equipped with a running wheel after their fur got dry in a new cage with fresh bedding chips. On the second day, tail suspension test (12:00–13:00) and treadmill test (15:30–18:30) were carried out. The video data saved was analyzed using an online/offline PC computer system (O'Hara & Co.).The analyses were performed practically in a blinded manner as for the state (depressive or euthymic).

Prediction of the occurrence of hypoactivity episode

The RSI indicator for daily wheel-running activity was used to predict the occurrence of hypoactivity episode. The prediction criteria are (1) RSI should be less than 25 at least for one day, and (2) RSI should be less than 50 for consecutive 5 days. We began the behavioral test battery within two days after the criteria were met. In general, however, we did not performed the behavioral test battery during the first predicted episode of each animal, because some, but few, of mice (~5%, regardless of genotype) became chronically hypoactive after they exhibited robust wheel-running activity for 1–2 months and the prediction criteria were met at the transition phase. In our experience, mice that actively ran on a wheel for more than three months did not become chronic hypoactivity afterward. So, four months after we started measuring the wheel-running activity, we performed the test battery during the first predicted episode.

Open-field test

Each mouse was placed gently near one corner of the open-field arena (60 cm × 60 cm)

(O'Hara & Co.). The color of the floor and walls (30 cm high) was gray. A white LED-based planar lighting was placed on the ceiling (75 cm from the arena floor) and was set to 70 lux at the center of the open-field arena. Spontaneous behaviors of mice in the arena were videotaped for 15 min using a CCD camera mounted on the ceiling.

Y-maze test

The maze consisting of three arms was made of gray PVC material; each arm was 40 cm long, 12 cm high, 3 cm wide at the bottom, and 11.5 cm wide at the top (O'Hara & Co.). A white LED-based planar lighting was placed on the ceiling (75 cm from the bottom of the maze) and was set to 5 lux at the floor level. Each mouse was placed in the middle of an arm and in the direction of the tip of the arm. Mice sequentially explored three arms of the Y maze. Spontaneous behaviors of mice in the arena were videotaped for 15 min using a CCD camera mounted on the ceiling. Time spent in the center of the Y maze at the junction of the three arms was measured as an index of indecisiveness. A few mice (2 in 12 mutant mice during episodes and 4 in 13 mutant mice in non-episode) did not explore the maze, and they were excluded from the statistical analysis.

Forced swimming test

Each mouse was placed in a transparent, acrylic glass cylinder (11 cm diameter $\times$ 21.5 cm height) filled with 11.5 cm of tap water (22.5 °C $\pm$ 0.5 °C) where it could not touch the containers floor (O'Hara & Co.). The cylinder was placed in an opaque box (33 cm $\times$ 22 cm $\times$ 48 cm). Behaviors of mice were videotaped for 6 min using a CCD camera mounted in the box.

Tail suspension test

Each mouse was suspended by its tail which, ~1 cm from the base, was attached to a small aluminum plate with adhesive medical tape, and the plate was hooked to an attachment located inside an opaque box (48 $\times$ 22 $\times$ 33 cm) (O'Hara & Co.). The distance between the tip of the nose of each mouse and the floor was ~15 cm. Behaviors of mice were videotaped for 6 min using a CCD camera mounted in the box.

Treadmill test

Each mouse was placed on a treadmill belt with electric grids (0.2 mA) at the rear of the treadmill (Panlab, Barcelona, Spain) at a constant 25° angle. Running speed was gradually increased by 1 m/min every 1 min from an initial speed of 5 m/min until exhaustion, which was defined as the point at which the mouse could no longer run on the treadmill to avoid a shock from the grids for more than 3 s.

Sucrose preference test

After recording the wheel-running activity for several months, 29 female *Polg1* mutant mice were given a free choice between two bottles, one with 0.75% sucrose solution and another with water. The mice were continuously housed in cages with a wheel. To control for side preference in drinking behavior, the position of the bottles was switched every 24 h. The consumption of water and sucrose solution was measured by weighing the bottles every day at the same time of the day for 30 consecutive days. The preference for sucrose was calculated as a percentage of consumed sucrose solution of the total amount of liquid drunk.

Long-term recording of wheel-running speed

The above-mentioned apparatus for measuring wheel-running activity (O'Hara & Co.) was improved to record the activity by the 0.1 rotation/s. We tested 12 *Polg1* mutant mice and their feces were collected for corticosterone assay.

5-Choice serial reaction time task (5-CSRTT)

We used a mouse operant chamber (O'Hara & Co.) equipped with five nose-poke holes on a curved wall in the front. On the opposite wall, there was a pellet dispenser that delivered food reward (10-mg pellet, TestDiet, St. Louis, MO, USA). Each chamber was installed in an independent soundproof box with a white house light on the ceiling.[37] Training and test procedures of 5-CSRTT and a method for simultaneous wheel running were as follows: Female mice were individually housed in cages equipped with a running wheel. After three weeks, food restriction began and reduced their body weight to approximately 85% of free-feeding weight in the following week. Wheel running activity was continuously measured. In the next week, the mice were habituated for the chamber for 30 min (2 days) and trained to retrieve food pellets from the pellet dispenser for 30 min (4 days). Twenty trials were given at 45-s intervals. The seventh day was a rest day. The mice were then trained to associate nose-pokes with food in a non-specific manner in the next two weeks. This training session ended after 100 trials or 30 min. The inter-trial interval (ITI) was 2 s, and the limited hold (LH) of the cue lights behind all of the holes was 60 s. The seventh and 14th days were rest days. The mice were then trained to detect the presentation of a random cue light at one of five spatial locations for two weeks. Initially, the ITI was 2 s, the LH was 30 s, and the duration of extinction of the house light (time-out) was 2 s. These were gradually adjusted across training session to the durations for the test session. This training session ended after 100 trials or 30 min. The seventh and 14th days of the final training phase were rest days. In the following three weeks, the mice were tested using the test procedure of 5-

CSRTT, which was as described in the final training phase with the ITI of 10 s, the LH of 15 s, the time-out of 2 s. The seventh and 14th days of the test phase were rest days. All of the mice, both Tg and non-Tg mice, showed an accuracy (the percentage of correct responses) of more than 80% after the test phase. On the 27th day, the mice were given a plenty of food after the test session. The mice run on a wheel for a week without food restriction. Then the mice were fasted for about 24 h to lose weight approximately 15%, tested using the test procedure of 5-CSRTT, and given a plenty of food. This weekly test of 5-CSRTT was performed for 26 weeks.

Pup retrieval assay

Nulliparous, virgin female mice were individually housed in cages (24 cm × 14 cm) with running wheels. We recorded the wheel-running activity for 25 weeks as described above and performed a pup retrieval assay when an animal exhibited episodic hypoactivity. Tg littermates in euthymic state and non-Tg littermates were also tested as controls. Each animal was exposed to three 1- or 2-day-old pups, which were taken from unrelated C57BL/6J dam(s). Before placing pups, we identified on which side of the cage the mouse made the nest, and three pups were placed on the side of the cage opposite to the nest. We continually observed the behavior of the female mice for 20 min and recorded the latencies to sniff a pup for the first time and to retrieve each pup into the nest. Only pups brought completely into the nest were counted as retrieved. If a pup was transported into the running wheel during the test, the pups were immediately plucked from the wheel and placed on the bedding chips again.

Light/dark transition test

The light/dark box consisted of a light chamber which was made of white ABS plastic (20 × 20 × 25cm) and illuminated by white LED lights (200 lux at the center of the box) and an equal-sized bark chamber which was made of black ABS plastic (< 1 lux) (O'Hara & Co). There was a small opening (3 × 5 cm) on the partition between the light and dark chambers. Each mouse was placed into the light chamber and then allowed to move freely in the light and dark chambers for 10 min, which was videotaped using infrared CCD cameras mounted on the ceilings.

Comprehensive mapping of Δ-mtDNA accumulation

After decapitation, brains of *Polg1* mutant mice and wild-type controls were immediately dissected and frozen in Tissue-Tek OCT 4583 compound (Sakura, Tokyo, Japan). The frozen blocks were sectioned on a cryostat (Leica Microsystems, Nussloch, Germany) to a thickness of 40 µm. Sections were briefly fixed in 70% EtOH for 15 s, washed in nuclease

free water for 10 s and stained in 0.05 % toluidine blue solution (pH 4.1) for 30 s. Sections were washed in nuclease free water again and air dried. After taking pictures of each stained section, deep staining with eosin-Y solution (10 min) was additionally performed, in order to achieve a sharp laser focus that enable us to perform laser capture microdissection (LCM) with lower energy and obtain samples with better quality. Designs of cut lines, laser microdissection, and laser pressure catapulting were performed using PALM MicroLaser system (PALM, Bernried, Germany). Microdissected pieces were captured into a 96-well PALM CapturePlate. For sagittal sections, 20 × 40 grid lines covering the whole brain section were designed (Figure 4a). For coronal sections, grid lines consisted of rectangle pieces sized 300 × 300 μm^2 were designed to cover whole hemisphere (Figure 4b). Captured pieces were incubated in a lysis buffer (20mM Tris-HCl, 0.25% NP-40, 0.25% Tween 20, 0.025% digitonin, 0.1 µg/µl Proteinase K; pH 8.0) at 37 °C for 16 h to extract total DNA. Amount of Δ-mtDNA in each piece was determined by qPCR using SYBR *Premix Ex Taq* Kit (Takara Bio, Otsu, Japan) with a primer pair (D3, 5´-CGA TAT ACA TAA ATG TAC TGT TGT ACT ATG-3´ and D4, 5´-AAC TCT AAT CAT ACT CTA TTA CGC-3´) as described previously.[18] After an initial denaturation step (95 °C for 1 min), PCR amplification proceeded for 40 cycles (95 °C for 20 s; 55 °C for 30 s; 72 °C for 90 s). Quadruplicate aliquots of the DNA sample extracted from one LCMed piece were PCR amplified using 7900HT Fast Real-Time PCR System (Life Technologies, Carlsbad, CA, USA). A median of the threshold cycles *Ct*(Δ-mtDNA) was calculated to determine the amount of Δ-mtDNA in each piece by comparing the *Ct*(Δ-mtDNA) to a standard curve, which was made in the same plate using standards serially diluted from a stock solution containing a known amount of Δ-mtDNA. The standards were prepared as follows: Δ-mtDNA molecules were PCR amplified using total DNA extracted from the cortex of *Polg1* mutant mouse as a template. The PCR product was purified and quantified by UV spectrophotometry. This Δ-mtDNA solution was diluted using total DNA extracted from brain of a young WT mouse, which contained negligible amount of Δ-mtDNA and a similar amount of molecules that could interfere with PCR as the DNA extractions from LCMed pieces. According to the amount of Δ-mtDNA in each piece, the following colors were overlaid on the figure of the slice: $\geq 2^{-2}$ fg, red; 2^{-2}–2^{-3} fg, orange; 2^{-3}–2^{-4} fg, light orange; 2^{-4}–2^{-5} fg, gold; 2^{-5}–2^{-6} fg, yellow; $< 2^{-6}$ fg, no color; data not determined, gray. Amount of total mtDNA in each piece was evaluated by qPCR using the SYBR *Premix Ex Taq* Kit with a primer set designed on *Nd4* coding sequences (5´-CAT CAC TCC TAT TCT GCC TAG CAA-3´ and 5´-AGT CCT CGG GCC ATG ATT ATA GT-3´) and the following thermal cycling protocol: 95 °C for 5 s, 60 °C for 30 s for 40 cycles. For each piece, quadruplicated experiments were performed and the median *Ct* was used as the representative value

(*Ct*(*Nd4*)). The amount of Δ-mtDNA normalized by the amount of total mtDNA was calculated as $2^{(Ct(Nd4) - Ct(\Delta\text{-mtDNA}))}$. If the *Ct*(Δ-mtDNA) or the *Ct*(*Nd4*) was not determined in the qPCR of 40 cycles, *Ct* was set to 40. The ages of the mice used were 85-weeks old for the quantitative mapping of Δ-mtDNA (sagittal sections), 96- and 101-weeks old for the quantitative mapping of Δ-mtDNA (coronal sections), 96–102-weeks old (99.2 ± 2.9) for the ROI analysis, and 101–116-weeks old (108.7 ± 7.5) for the expression analysis of mut*Polg1* transgene and wild-type *Polg1* mRNA.

Δ-mtDNA quantification in regions of interest

According to the results of the quantitative mapping of Δ-mtDNA, we selected 22 regions of interest (ROIs) comprising the brain regions where high levels of Δ-mtDNA accumulation was detected in the comprehensive mapping of Δ-mtDNA accumulation (high Δ-mtDNA regions) and quantifiable amount of Δ-mtDNA was largely not detected (low Δ-mtDNA regions). Each ROI was defined as described in Supplementary Figure 6. To avoid any arbitrariness, ROI definitions were based on clear cytoarchitectural differences. For Δ-mtDNA quantification in each ROI, grid-shaped cut lines consisted of rectangle pieces sized 300 × 300 μm^2 were designed to cover the defined area. The amount of Δ-mtDNA relative to total mtDNA in each piece was calculated by the methods described above, and the average for five *Polg1* mutant mice was determined.

Expression analysis of mut*Polg1* transgene and endogenous wild-type *Polg1*

Microdissected tissue samples of eight brain regions (IL, S1, NAc, CP, PVT, LTR, cDG and rDG) were prepared according to the methods described above, and definition of ROIs is shown in Supplementary Figure 6. For each ROI, tissues from 2–8 consequent sections were corrected and total RNA was extracted from these samples using the RNeasy Micro Kit (Qiagen, Venlo, Netherlands) following the manufacturer's instructions with some modifications. Complementary DNA was synthesized from total RNA using the Superscript III reverse transcriptase (Life Technologies) with oligo(dT) primer. Expression levels of mutant and wild-type *Polg1* were evaluated by qPCR using the SYBR *Premix Ex Taq* Kit. The primer sets used were designed to amplify the mut*Polg1* transgene-specific sequence and the wild-type *Polg1*-specific 5' untranslated sequence (mut*Polg1*; 5´-GGC ATG ACT TCT GCG CTA A-3´ and 5´-GAT TGT CTT TTC TGA CCA GAT GG-3´, wild-type *Polg1*; 5´-AGC TTG ACT GCT TTT AGT GGC-3´ and 5´-GCC GCA GAA CGG GAA G-3´). The thermal cycling protocol used was 95 °C for 20 s, 55 °C for 30 s, 72 °C for 60 s for 40 cycles. For each sample, quadruplicated experiments were performed and the median *Ct* was used as the representative value.

Immunohistochemistry of mouse brain samples

Mice were deeply anesthetized by intraperitoneal administration of 2.5% avertin (Tribromoethanol) at a dosage rate of 0.2 mL/10 g body weight and perfused transcardially with 4% paraformaldehyde (PFA) in phosphate-buffered saline (PBS). Brain tissues were isolated, post-fixed in 4% PFA for one or two overnights and embedded in paraffin or OCT compound (Sakura) for cryosections. Paraffin sections (8 μm thickness) were mounted on glass slides and deparaffinized with xylene. For COX/SDH immunofluorescent staining, the sections were placed in methanol for 30 min at room temperature (RT), then dried, and incubated with 0.1% Triton-X in PBS for 30 min. The specimens were heated with an antigen retrieval solution (100 mM Tris-HCl, 5% urea, pH 9.5) at 95 °C for 10 min. After rinsing with PBS, the sections were treated with Mouse Ig Blocking Reagent (Vector Laboratories, Burlingame, CA, USA) in PBS for 1 h at RT, rinsed with PBS, and treated with 10% normal goat serum in PBS for 1 h at RT. The sections were incubated with a mixture of monoclonal anti-MTCO1 (5 μg/mL; anti-complex IV subunit I (1D6E1A8); Life Technologies) and anti-SDHA (0.2 μg/mL; anti-complex II subunit 70kd Fp (2E3GC12FB2AE2); Life Technologies) antibodies in 10% normal goat serum in PBS at 4 °C overnight. After rinsing with 1% normal goat serum in PBS, the sections were incubated with a mixture of Alexa Fluor 488-conjugated goat anti-mouse IgG2a (2 μg/mL) and Alexa Fluor 568-conjugated goat anti-mouse IgG1 (2 μg/mL) antibodies in 10% normal goat serum in PBS for 2 h at RT. After rinsing with 1% normal goat serum in PBS, cover slips were mounted on the glass slides using a fluorescent mounting medium containing 4´,6-diamidino-2-phenylindole (DAPI) and sealed with nail polish. For characterization of COX-negative cells, triple immunofluorescent staining with COX/SDH was performed by using rabbit anti-Calretinin (Spring Bioscience, Pleasanton, CA, USA), rabbit anti-GFAP (DAKO, Glostrup, Denmark), or rabbit anti-Iba1 (Wako pure chemical industries, Osaka, Japan) antibody. For GFP and VAMP2 staining in the AAV infection experiment, rat anti-GFP (Nacalai Tesque, Kyoto, Japan) and rabbit anti-VAMP2 (Synaptic Systems, Goettingen, Germany) antibodies were used. GFP signal was amplified by 10-min treatment of biotin-tyramide (PerkinElmer, Waltham, MA, USA) with Alexa Fluor 488-conjugated streptavidin (Life technologies). GFP signals derived from the transgene of Tg3-TeTX could not be detected as previously described.[19] Fluorescence images were captured with a multi-dimensional time-lapse imaging system (ZDC-IMAGE, Olympus, Tokyo, Japan) or with confocal microscopy (FV1000, Olympus) and acquired with MetaMorph software (Molecular Devices, Sunnyvale, CA, USA). The merged images of the anterior part of the brains were processed with photomerge command in Photoshop CS4 (Adobe Systems, San Jose, CA, USA).

Activity staining of COX/SDH

Mice were sacrificed by decapitation, and brains were isolated and frozen in acetone/dry ice. Sections (8 μm thickness) were mounted on glass slides and stored at −80 °C. After rinsing with PBS at RT, the sections were incubated in COX-staining solution (0.25 mg/mL 3,3´-diaminobenzidine (DAB), 2 mg/mL catalase, 1 mg/mL cytochrome *c*, 75 mg/mL sucrose, in 0.05 M phosphate buffer; pH 7.4) at RT for 30 min. After rinsing with PBS at RT, the sections were incubated in SDH-staining solution (1 mg/mL nitro blue tetrazolium chloride, 54 mg/mL sodium succinate in 0.2 M phosphate buffer; pH 7.4) at 37 °C for 60 min. The sections were rinsed with DDW, then with 30%, 60%, 90%, 60%, and 30% acetone in DDW, and again with DDW. Cover slips were mounted on the glass slides using an aqueous mounting medium (Aquamount; Polyscience, Warrington, PA, USA) and sealed with nail polish. Images were obtained by Leica biological microscope DM6000M (Leica Microsystems).

Quantification of Δ-mtDNA in LCMed neurons

To detect COX-negative neurons, COX activity staining was followed by Nissl staining by thionin. Although COX/SDH activity staining is widely used for identification of COX-negative cells, Kraytsberg *et al.*[38] previously mentioned that combined COX activity and Nissl staining is able to reveal more COX-negative neurons than COX/SDH activity staining. Mouse brain frozen sections (8 μm) were COX activity stained as described above, then stained with 0.25% thionin solution. Sections were dehydrated by acetone series: 30% (3 min), 60% (3 min) and 90% (5 min), and air dried. We microdissected COX-negative cells from the PVT of each *Polg1* mutant mouse, and COX-positive cells from the PVT and a control region (VL) of mutant mice and control mice. Because the VL contained fewer COX-negative cells, we used the region as a control. Hundred individual COX-negative or -positive cells identified by color (blue and brown, respectively) were collected in a 0.5 ml tube for each sample using a PALM microscope. The cells were incubated in 40 μL of a lysis buffer (0.05% Triton X-100, 0.5 mg/mL Proteinase K in TE buffer; pH 8.0) at 37°C for 12 h to extract total DNA. In dissected cells, we assessed the amount of Δ-mtDNA by real-time qPCR using QuantiTect Multiplex PCR Kit (Qiagen) according to manufacturer's instructions. The amount of Δ-mtDNAs was determined from the copy number ratio of two mtDNA segments, the *mt-Co1* and D-loop region, which were lost and preserved in Δ-mtDNAs, respectively. The PCR primers and TaqMan MGB probes (Life Technologies) used in the assay are follows: for *mt-Co1*, forward primer 5´-AAC CCC CAG CCA TAA CAC AG-3´, reverse primer 5´-GTA TAG TAA TGC CTG CGG CTA GC-3´, probe (FAM-dye labeled) 5´-CCG TAC TGC TCC TAT-3´; for D-loop (control region),

forward primer 5´-CCC TCC TCT TAA TGC CAA AC-3´, reverse primer 5´-TGA TCA GGA CAT AGG GTT TGA TAG-3´, probe (VIC-dye labeled) 5´-AAC ACT AAG AAC TTG AAA GAC-3´. The relative amount of Δ-mtDNA was calculated by comparative Ct method (ΔΔCt method). Brains of the three female *Polg1* mutant mice (113–116 weeks old) and three control littermates were used for this assay. An 8-week-old female non-Tg mouse brain was used as control.

Postmortem human brain samples

Formalin fixed, paraffin embedded human postmortem brain tissues of patients with mitochondrial diseases and controls were selected from among the brain tissue resource in Niigata University Brain Research Institute and Osaka Red Cross Hospital (Case 1 only).

Case 1 is 66-year-old female diagnosed as CPEO. She presented bilateral ptosis at age 48 and gradually developed muscle weakness. At age 56 she was referred to a neurologist and diagnosed as having ophthalmoplegia, muscle weakness and sensorineuronal hearing loss. Skeletal muscle biopsy showed ragged-red fibers, COX-negative fibers, and multiple mtDNA deletions. At age 57, she showed Parkinsonism and gradually developed severe depression, suicidal idea, hallucination, and delusions. She died of pneumonia at the age of 66.

Case 2 is 58-year-old male diagnosed as Kearns Sayre syndrome (KSS); a severe form of CPEO. He developed bilateral visual loss since age 15 and diagnosed as retinal pigment atrophy at age 35. He developed external ophthalmoplegia, muscle atrophy, cerebellar ataxia and mood symptoms such as euphoria and irritability, at age 56. He also showed seizures and bizarre behavior at age 58. He showed increase of lactate and pyruvate in cerebrospinal fluid. He died at age 58 due to gastric cancer.

Control subjects were two subjects (1 male and 1 female) aged 51 and 63 years old, who did not have remarkable central nervous system diseases.

COX/SDH immunohistochemistry in postmortem human brain samples

Sections (4 μm thickness) including thalamus of patients with KSS and CPEO, and those of control subjects were processed as described above with slight modifications. For samples of a patient with KSS and age-matched controls, the primary antibodies were applied at the concentration of 10 μg/mL of anti-MTCO1 and 0.4 μg/mL of anti-SDHA. Sections were pretreated with heat at 105 °C for 2 min for antigen retrieval. For samples of a patient with CPEO and an age-matched control, sections were incubated with 0.8% BlockAce (Dainippon-Sumitomo pharma, Osaka, Japan) in PBST (0.01% Tween 20 in PBS) before treatment with the primary antibodies to reduce background auto fluorescence. The sections were pretreated with heat at 121 °C for 10 min for antigen retrieval to get enough

signals. The primary antibodies were used at the higher concentration [anti-MTCO1 (10 μg/mL) and anti-SDHA (4 μg/mL)]. A mixture of Alexa Fluor 488-conjugated goat anti-mouse IgG2a (4 μg/mL) and Alexa Fluor 647-conjugated goat anti-mouse IgG1 (4 μg/mL) antibodies were used as secondary antibodies. Negative controls were processed in parallel by using a diluted reagent without primary antibodies under the same condition. The images were scanned and analyzed using a digital pathology system (NanoZoomer 2.0-RS, Hamamatsu Photonics, Hamamatsu, Japan).

Virus production and injection into the mouse PVT

For region-specific inhibition of neural transmission, we generated a recombinant AAV expressing Cre recombinase and EGFP bicistronically. A fragment containing Cre-IRES-EGFP was amplified by PCR from pCAG-Cre-IRES-EGFP plasmid (Addgene, Cambridge, MA, USA). This fragment was subcloned under the pCMV-β globin intron driver of AAV MCS vector to obtain pAAV2 Cre IRES EGFP. AAV particles were produced by using HEK293 cell transfection protocol.[39] For the injection of AAV into the PVT, female mice (heterozygous double-Tg mice Tg2/;Tg3/+ or the other littermate controls, 24–33 week old) were anesthetized with isoflurane and fixed in a stereotaxic frame. The AAV (0.5–1.0 μL) was injected at AP −1.7 mm, ML 0.0 mm, and DV 3.2 mm from the bregma by using a pump (UMP3; World precision instruments, Sarasota, FL, USA) with a 10-μL Hamilton syringe attaching a 33-gauge needle.

Statistics

The results of quantitative experiments were analyzed by parametric tests after a test for equality of variances or a Kolmogorov-Smirnov test for confirmation of a normal distribution. Nonparametric tests were also used when they are appropriate. A two-tailed test was used for exploratory analysis. Whenever one-tailed test is used, it is described as such. Statistical analyses were performed using SPSS 18.0 (SPSS, Chicago, IL, USA), KyPlot 4.0 (KyensLab, Tokyo, Japan), Excel 2003, 2007, 2010, 2013 (Microsoft, Redmond, WA, USA), or R (R Development Core Team). Sample power was calculated using G*power software (UCLA Statistical Consulting Group) or R. The sample size of the wheel-running analysis (67 Tg and 28 non-Tg mice) showed *post hoc* statistical power of 99% at alpha error probability of 0.05 and effect size *d* of 1. The sample size of the other behavioral analyses including functional PVT knock down experiment was in principle set at $n = 13$ in each group. This was decided *a priori* to achieve the statistical power of 65% (for two-sample t-test) at alpha error probability is 0.05 and the effect size *d* is 1. Thus, there was a relatively large possibility of type II error to overlook the existing difference. The sample size of escitalopram experiment was determined to be $n = 14$ for each group by a statistical

power analysis ($\alpha = 0.05$ and power ($1-\beta$) at 90%) assuming that the Tg mice experience episodes once per half year and the drug completely inhibits the episode (Fisher's exact probability test).

The sample size of the COX/SDH immunofluorescent staining (7 Tg and 6 non-Tg mice) showed *post hoc* statistical power of 99% (for two-sample *t*-test) at alpha error probability of 0.05 and effect size *d* of 2.1. The sample size of the quantification of Δ-mtDNA in brain ROIs (5 Tg mice) showed *post hoc* statistical power of 99% (for paired *t*-test) for most of brain regions at alpha error probability of 0.05 and effect size *d* of 3 or more. The sample size of the quantification of Δ-mtDNA in LCMed neurons (3 Tg and 3 non-Tg mice) showed *post hoc* statistical power of 87% (for two-sample *t*-test) at alpha error probability of 0.05 and effect size *d* of 2.8 for the comparison of COX-negative cells of Tg versus VL of non-Tg. Decrease of sample size due to unpredicted drop of mice caused increased chance of type II error. Because of the difficulty of the experiments, however, we employed this sample size.

Supplementary References

35. Wilder JW. *New Concepts in Technical Trading Systems*. Trend Research: Greensboro, 1978.

36. Touma C, Palme R, Sachser N. Analyzing corticosterone metabolites in fecal samples of mice: a noninvasive technique to monitor stress hormones. *Horm Behav* 2004; **45:** 10–22.

37. Kobayashi Y, Sano Y, Vannoni E, Goto H, Suzuki H, Oba A *et al.* Genetic dissection of medial habenula-interpeduncular nucleus pathway function in mice. *Front Behav Neurosci* 2013; **7:** 17.

38. Kraytsberg Y, Kudryavtseva E, McKee AC, Geula C, Kowall NW, Khrapko K. Mitochondrial DNA deletions are abundant and cause functional impairment in aged human substantia nigra neurons. *Nat Genet* 2006; **38:** 518–520.

39. Yagi H, Ogura T, Mizukami H, Urabe M, Hamada H, Yoshikawa H *et al.* Complete restoration of phenylalanine oxidation in phenylketonuria mouse by a self-complementary adeno-associated virus vector. *J Gene Med* 2011; **13:** 114–122.

Supplementary Table S2.

Comparison of the episode-specific phenotypes of *Polg1* mutant mice with the DSM-5 criteria for major depressive episode.

Criteria A Five (or more) of the following symptoms have been present and represent a change from previous functioning; at least one of the symptoms is either (1) depressed mood or (2) loss of interest or pleasure.
(1) Depressed mood.
✗ As a self-reported criterion, this was unable to be assessed in the mouse.
(2) Loss of interest or pleasure.
✓ The reduction in wheel running indicated lethargy with a possible loss of hedonic interest during the hypoactivity episode. Wheel running has been shown to activate reward circuit like drugs of abuse[26] in contrast to other forms of locomotion, which were not affected during the episodes (Figure 3a and Supplementary Figure 3c).
(3) Weight loss or weight gain, or appetite change.
✓ The mutant mice displayed a marked weight gain and increased food intake during the episodes (Figure 3b−d)
(4) Insomnia or hypersomnia.
✓ EEG/EMG recordings revealed significant sleep disturbances (Figure 2c and d)
(5) Psychomotor agitation or retardation.
✓ A measurable slowing of running speed during the episodes suggested psychomotor retardation (Figure 3g and h).
(6) Fatigue or loss of energy.
✓ The treadmill test showed that mutant mice had fatigue during the episodes (Figure 3i).
(7) Feelings of worthlessness or excessive or inappropriate guilt.
✗ As self-reported criteria, this could not be examined in the mouse.
(8) Diminished ability to think or concentrate, or indecisiveness.
✗ This symptom was not observed in the 5-CSRTT or Y-maze test (Supplementary Figure 4a–c).
(9) Suicidality.
✗ This could not be assessed in the mouse.
Criteria B The symptoms cause clinically significant distress or impairment in social, occupational or other important areas of functioning.
✓ In the pup retrieval assay, the mutant mice during the episodes had impaired maternal behavior (Figure 3j), which is one of the most important social functions of female mice.

Supplementary Table S3.

Abbreviations for anatomical regions.

Abbreviation	Name
PL	prelimbic cortex
IL	infralimbic cortex
Ins	insular cortex
LS	lateral septum
NAc	nucleus accumbens
BNST	bed nucleus of the stria terminalis
PVT	paraventricular thalamic nucleus
EP+	endopiriform nucleus
dEnt	entorhinal area, deep layer
BA	basal amygdala
cDG	dentate gyrus, caudal part
vEnt	entorhinal area, ventral part
Ect	ectorhinal area
M1	primary motor cortex
S1	primary somatosensory cortex
MHR	midline hypothalamic region
rDG	dentate gyrus, rostral part
LHR	lateral hypothalamic region
CP	caudate putamen
CA	corpus ammonium
Hb	medial habenula
LTR	lateral thalamic region
VL	ventral lateral nucleus of the thalamus
3V	third ventricle
EGP	external globus pallidus
IC	internal capsule
Pu	putamen

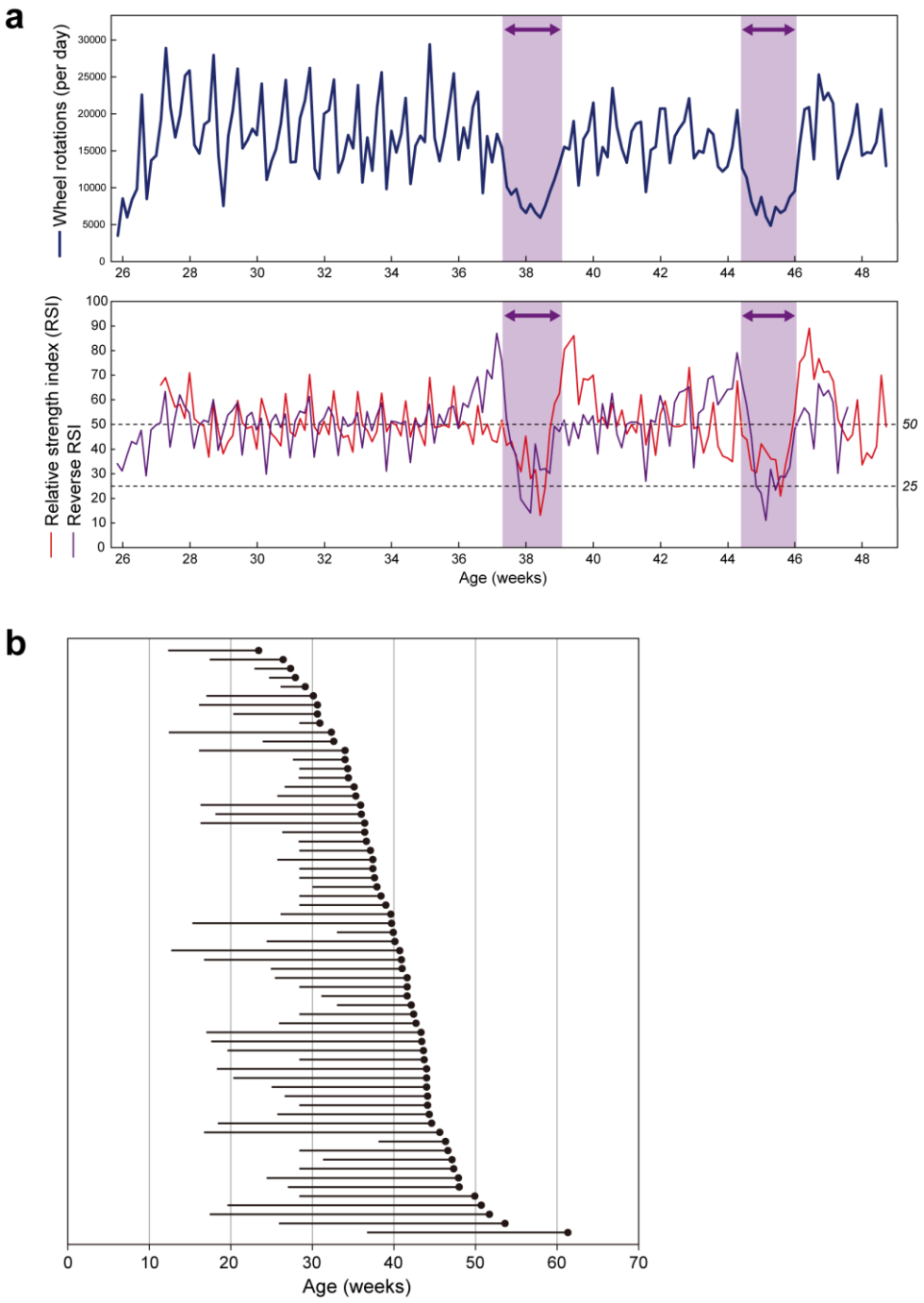

Supplementary Figure 1.

Definition of the hypoactivity episode and age-of-onset distribution.

(**a**) A representative recording of wheel-running activity of a female *Polg1* mutant mouse. Two hypoactivity episodes indicated by left-right arrows and purple backgrounds (upper). RSI and reverse RSI plots calculated from the wheel-running activity data (bottom). The operational criteria for the hypoactivity episode using the RSI (red line) are (1) RSI should be less than 25 at least for one day, and (2) RSI should be less than 50 for consecutive 9

days or more. The first day when RSI declined to less than 50 is defined as the onset of episode. The termination of episode is determined by “reverse RSI” (violet line). Although estrous cycle-associated activity change with a period of 4–5 days was manifest in euthymic state, it almost disappeared during episodes.
(**b**) Age-of-onset distribution of the hypoactivity episode in *Polg1* mutant mice. Horizontal bars denote duration from the beginning of wheel-running analysis to the onset of first episode of hypoactivity (closed circles). Each bar/closed circle represents an individual mouse. The age at first episode was generally 30 weeks old or older.

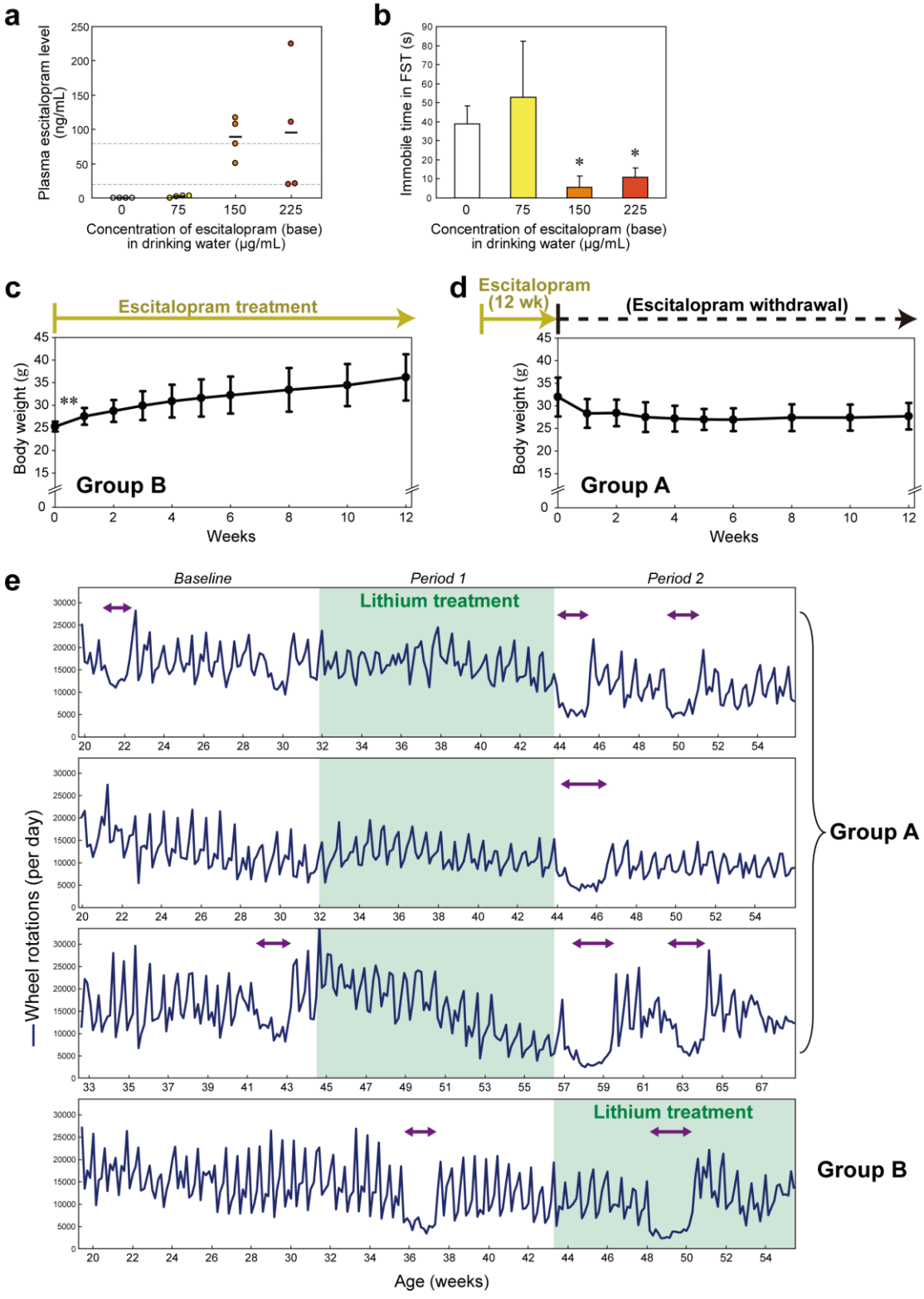

Supplementary Figure 2.

Effects of escitalopram and lithium treatments on *Polg1* mutant mice.

(**A**) A relationship between concentration of escitalopram in drinking water and plasma escitalopram level. We added escitalopram at various concentrations (0, 75, 150, 225

μg/mL) and gave them to female wild-type mice for 10 days. Although the therapeutic level in humans has not been established, plasma level of treated patients was 20–80 ng/mL. Two mice treated with escitalopram at the highest dose showed lower plasma levels probably due to less amount of drinking. At 150 μg/mL, chronic escitalopram treatment was sufficient to increase the plasma level in mice within the therapeutic range of depression patients treated with escitalopram.

(**b**) Effect of escitalopram in drinking water on immobility time in forced swimming test. Immobility time of mice treated with 150 or 225 μg/mL was dramatically and significantly decreased in comparison with untreated mice. $n = 4$ per group. $^{*}P < 0.05$ (Dunnett's test).

(**c,d**) Escitalopram treatment caused weight gain. (**c**) A significant increase in weight within one week after starting treatment. The body weight data were obtained from the *Polg1* mutant mice in Group B in Period 2 (Figure 1d). $^{**}P < 0.001$ (paired *t*-test). (**d**) The increased weight returned within one week after discontinuation of escitalopram treatment. The body weight data were obtained from the *Polg1* mutant mice in Group A in Period 2 (Figure 1d).

(**e**) Discontinuation of lithium treatment triggered hypoactivity episodes. Three representative recordings of *Polg1* mutant mice experiencing the hypoactive episodes after discontinuation of lithium. Relapses of mood episodes following discontinuation of lithium is well documented in patients with bipolar disorder (Suppes et al., 1991). Left-right arrows depict the duration of hypoactivity episode.

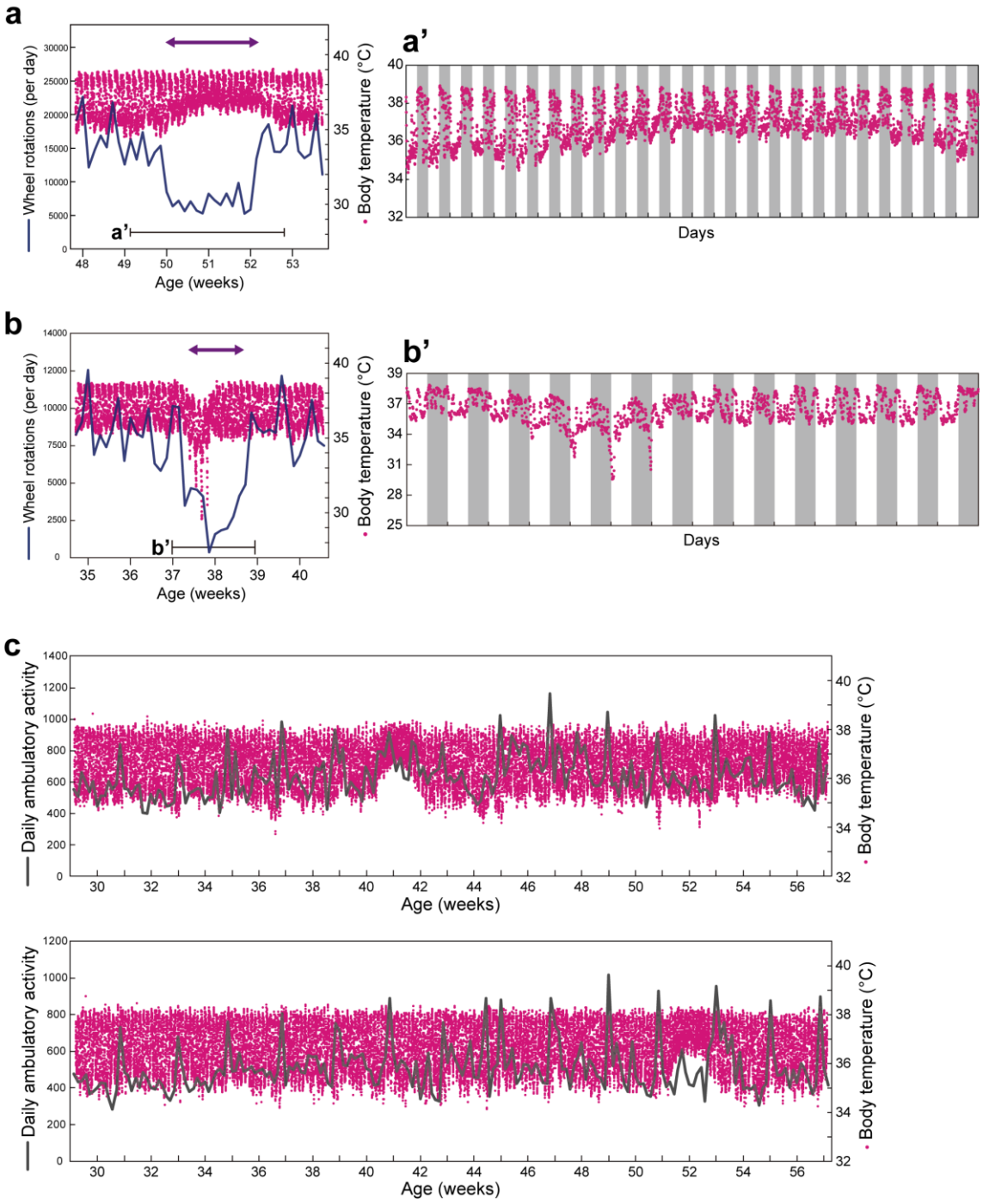

Supplementary Figure 3.

Long-term measurement of core body temperature of *Polg1* mutant mice.

(**a,b**) Alterations in body temperature during the hypoactivity episodes. (**a**) Diurnal body temperature was increased during the episodes. Core body temperature was measured every 10 min. A left-right arrow indicates the duration of the hypoactivity episode. An image enlarged along the temporal axis is shown in **a'**. The 12-h dark period is denoted by a gray background. (**b**) Anecdotal observation: a sharp drop of body temperature in the early

morning during the episode.

(**c**) Simultaneous measurement of ambulatory activity and body temperature of *Polg1* mutant mice housed in home cages without running wheels. Two representative recordings are shown. Daily ambulatory activity is expressed in arbitrary units. Ambulatory activity was recorded for 10 sec every 10 min and summed over one day. Transient peaks in daily ambulatory activity are obvious once every two weeks owing to replacement of the bedding and cage. Core body temperature was measured at 10-min interval. During the depression-like episodes indexed by increased body temperature, ambulatory activity in home cage was not altered.

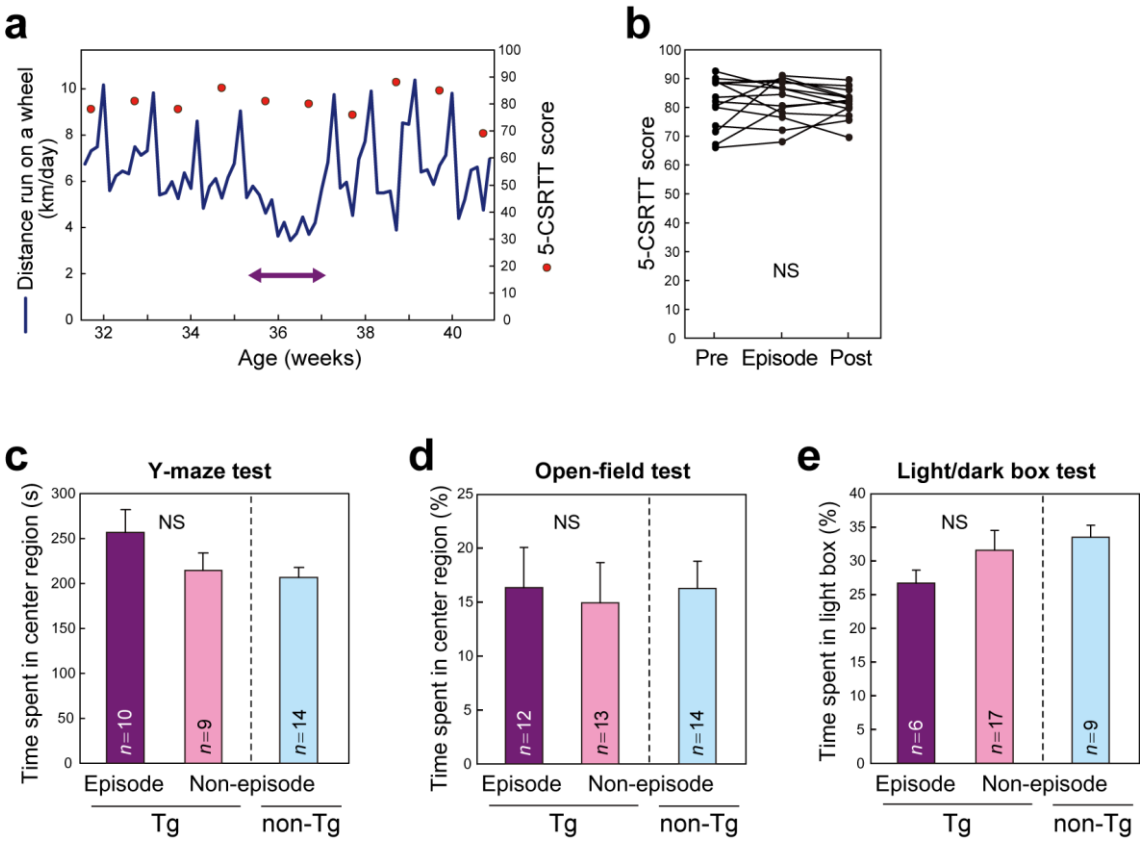

Supplementary Figure 4.

Assessment of attention/concentration, indecisiveness, and anxiety-like behavior of *Polg1* mutant mice during hypoactivity episodes.

(**a,b**) 5-CSRTT score reflecting the ability of concentration/attention of mice. (**a**) A representative recording. (**b**) Cumulative data for all episodes analyzed. There was no significant difference among the 5-CSRTT scores obtained before ("Pre"), during ("Episode"), and after ("Post") hypoactivity episodes (NS).

(**c**) Y-maze test. Time spent in the center region of Y maze is supposed to reflect indecisiveness of mice. There was no significant change between mutant mice during hypoactivity episodes and in non-episode periods (NS). Data for non-Tg mice were shown as a reference.

(**d,e**) Anxiety-like behavior assessed by open-field (**d**) and light/dark box (**e**) tests. There were no significant changes between mutant mice during hypoactivity episodes and in non-episode periods (NS). Data for non-Tg mice were shown as a reference.

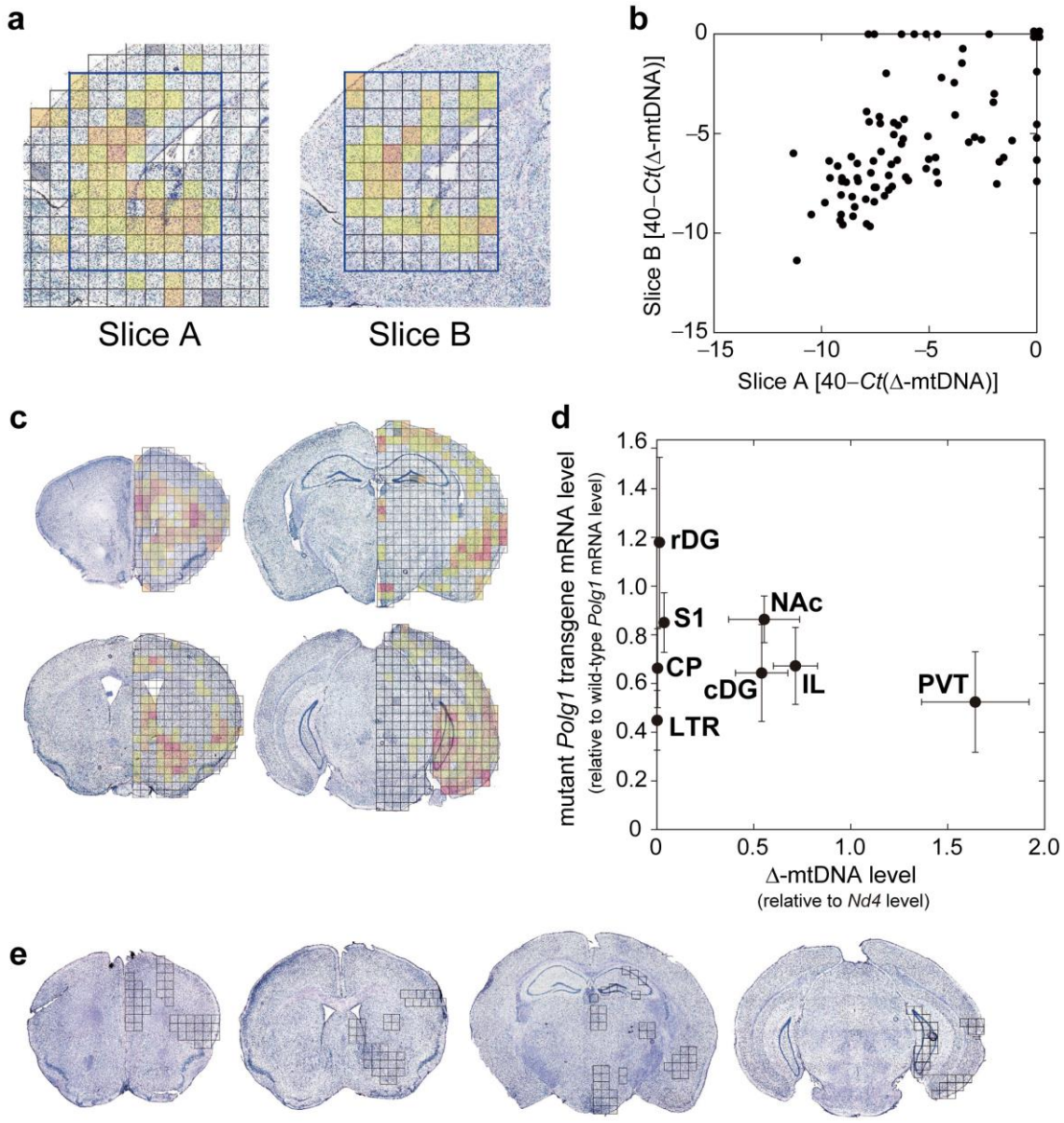

Supplementary Figure 5.

Quantitative mapping of Δ-mtDNA.

(**a**) Validation of quantitative mapping of Δ-mtDNA in the brain by comparing the data obtained from two adjacent sagittal sections (40 μm thickness). For slice B, only pieces shown with grids were analyzed. Levels of Δ-mtDNA are shown in the following colors: red (high), orange, light orange, gold, yellow (low), and no color (unquantifiable). Gray, data not determined. Each grid is 300 × 300 μm^2.

(**b**) A significant correlation between the data obtained from slice A and B (Pearson's r = 0.64, $P = 1.1 \times 10^{-22}$), supporting the reliability of the analysis.

(**c**) Levels of Δ-mtDNA accumulation in the left hemisphere of a 101-week-old male *Polg1* mutant mouse. The distribution pattern of Δ-mtDNA accumulation was similar to that in the

right hemisphere of a female *Polg1* mutant mouse shown in Figure 4b.
(**d**) Expression levels of mutant *Polg1* (mut*Polg1*) transgene mRNA and accumulation levels of Δ-mtDNA in *Polg1* mutant mice. Relationship between mutant *Polg1* transgene mRNA and Δ-mtDNA accumulation levels in four brain regions with high Δ-mtDNA levels (PVT, IL, NAc, and cDG) and four regions with low Δ-mtDNA levels (S1, rDG, CP, and LTR) (see Figure 4c). Expression levels of mutant *Polg1* transgene mRNA were normalized relative to endogenous wild-type *Polg1* mRNA levels and Δ-mtDNA levels were relative to Nd4 levels. Regional variation in the accumulation level of Δ-mtDNA did not correlate with regional variation in the expression level of the transgene. Rather, mutant *Polg1* mRNA level was inversely correlated with Δ-mtDNA level (Pearson's $r = 0.37$, $P = 0.052$). cDG, dentate gyrus, caudal part; CP, caudate putamen; IL, infralimbic cortex; LTR, lateral thalamic regions; NAc, nucleus accumbens; PVT, paraventricular thalamic nucleus; rDG, dentate gyrus, rostral part; S1, primary somatosensory cortex.
(**e**) Δ-mtDNAs were not detected in any brain sections, including in the PVT, of a control wild-type mouse at the age of two years. Only pieces shown with grids were analyzed. Δ-mtDNA accumulation was not detected in any pieces using the quantitative mapping method.

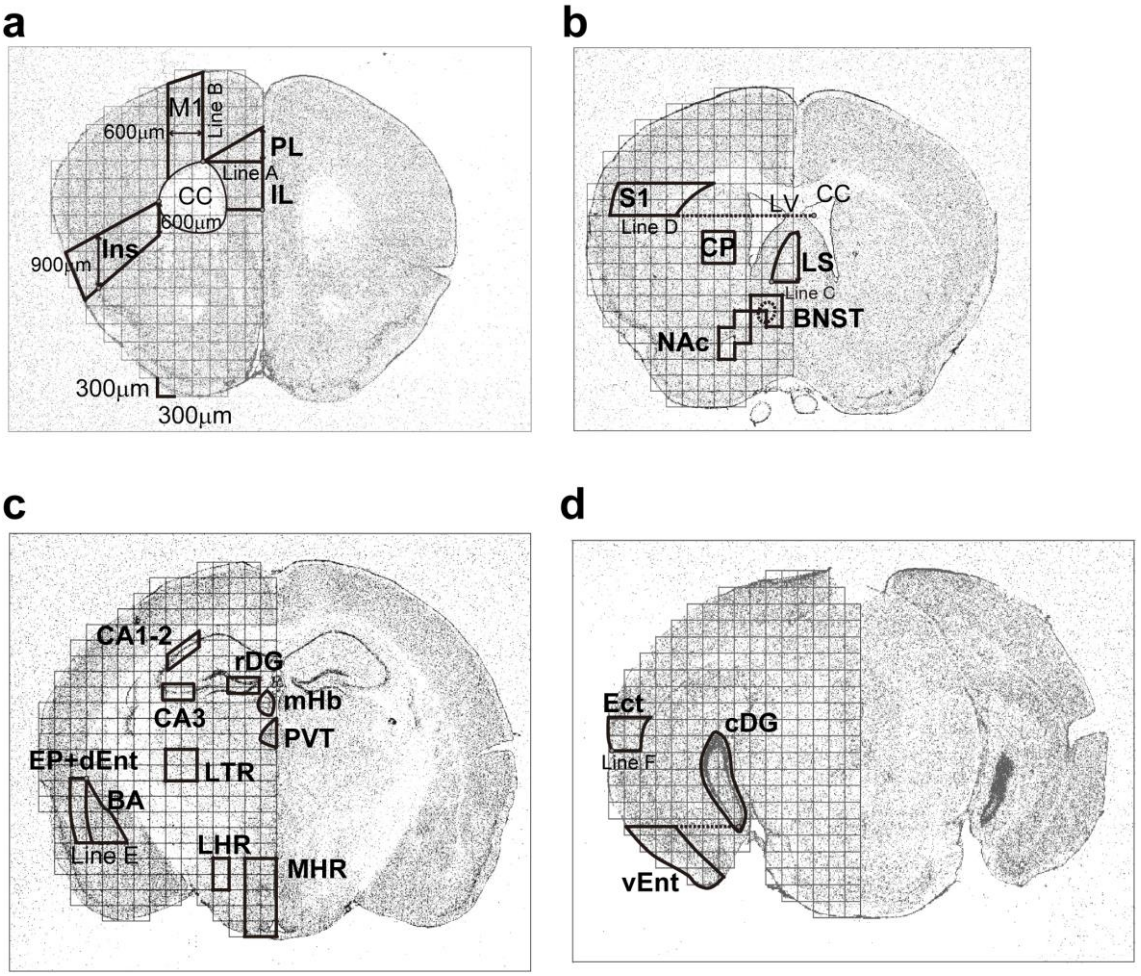

Supplementary Figure 6.

Definition of the brain regions used in the ROI analysis.

(**a**) The most anterior level. **IL, Infralimbic cortex**: This region was defined as the areas surrounded by these lines and curves: (i) the midline, (ii) a horizontal line passing through the dorsal end of the corpus callosum (CC) (line A), (iii) a horizontal line passing through the dorsal end of the bank of the dorsal peduncular area (DP) layer I, and (iv) the outer edge of the CC. **PL, Prelimbic cortex**: This region was defined as the areas surrounded by these lines: (i) the midline, (ii) line A, and (iii) a line passing through the dorsal end of the CC and a point 600 μm dorsal to the intersecting point of the midline and line A. **Ins, Insular cortex:** This region was defined as the areas surrounded by these lines and curves: (i) a line passing through a point 900 μm dorsal to the dorsal end of the pyramidal layer of the piriform area and the most lateral point of CC, (ii) a vertical line passing through the lateral end of the most lateral point of CC, (iii) a line passing through the point 600 μm ventral to the lateral end of the CC and the dorsal end of the pyramidal layer of the piriform area, and (iv) the outer edge of the brain. **M1, Primary motor cortex**: This region was

defined as the areas surrounded by these lines: (i) a vertical line passing through the dorsal end of the CC (line B), (ii) the parallel line 600 μm lateral to line B, (iii) the outer edge of the brain, and (iv) the outer edge of the CC.

(**b**) The second anterior level. **NAc, Nucleus accumbens**: Grid designs were placed to cover these regions according to the standard atlas. This region was defined as the Z or inverted Z shaped 4 pieces of tissues at the lateral side of the anterior commissure (dotted circle). **BNST, Bed nucleus of the stria terminalis:** Grid designs were placed to cover these regions according to the standard atlas. This region was defined as the 3 pieces of tissues at the medial, dorsal and dorsomedial side of the anterior commissure (dotted circle). **LS, Lateral septum**: This region was defined as the areas surrounded by these lines and curves: (i) the medial wall of the lateral ventricle (LV), (ii) a horizontal line passing through the ventral end of the LV (line C), (iii) a vertical line 300 μm lateral to the midline, and (iv) a horizontal line 900 μm dorsal to line C. **S1, Primary somatosensory cortex**: This region was defined as the areas surrounded by these lines and curves: (i) a horizontal line (line D) passing through a point where the corpus callosum (CC) intersects with the midline at the ventral side, (ii) a line parallel to and 600 μm dorsal from line D, (iii) the dorsal edge of CC, and (iv) the outer edge of the brain. **CP, Caudate putamen**: A 600 × 600 μm^2 of square-shaped area that definitely includes this region was defined according to the standard atlas.

(**c**) The second posterior level. **BA, Basal amygdala**: This region was defined as the areas surrounded by these lines and curves: (i) the amygdalar capsule, (ii) the external capsule, (iii) a horizontal line 1,200 μm ventral from the bifurcation of the amygdalar capsule and the external capsule (line E). **EP+dEnt, Endopiriform nucleus + Entorhinal area, deep layer**: This region was defined as the areas surrounded by these lines and curves: (i) the external capsule, (ii) a curve parallel to and 300 μm lateral from the external capsule, (iii) line E, and (iv) a horizontal line passing through the bifurcation of the amygdalar capsule and the external capsule. **PVT, Paraventricular thalamic nucleus**: The midline thalamic region with apparently higher cell density compared to adjacent thalamic regions was defined as this nucleus. **mHb, Medial habenula**: As this region has an unambiguous structure, it was defined according to the standard atlas. **MHR, Midline hypothalamic region**: A 1,500 × 600 μm^2 of square-shaped area in the most medial and ventral part of the hypothalamus, which would include the dorsomedial hypothalamic nucleus. **CA1-2, CA3, and rDG, dentate gyrus, rostral part**: As these regions have unambiguous structures, they were defined according to the standard atlas. Every piece was designed to contain the granular layer. **LTR, Lateral thalamic region**: A 600 × 600 μm^2 of square-shaped area at the medial side of the internal capsule are defined according to the standard atlas. **LHR, Lateral hypothalamic region**: A 600 × 300 μm^2 of square-shaped

area at the medial side of the internal capsule are defined according to the standard atlas. (**d**) The most posterior level. **cDG, Dentate gyrus, caudal part**: As this region has an unambiguous structure, it was defined according to the standard atlas. The area surrounded by the line approximately 100 μm outer from the lateral edge of the granular layer of the dentate gyrus was defined as this region. **vEnt, Entorhinal area, ventral part**: This region was defined as the areas surrounded by these lines and curves: (i) the external capsule, (ii) a horizontal line passing through the ventral end of the granular layer of the dentate gyrus, and (iii) the outer edge of the brain. **Ect, Ectorhinal area**: This region was defined as the areas surrounded by these lines and curves: (i) the external capsule, (ii) a horizontal line passing through the small dimple on the perirhinal area (line F), (iii) a line parallel to and 600 μm dorsal from line F, and (iv) the outer edge of the brain.

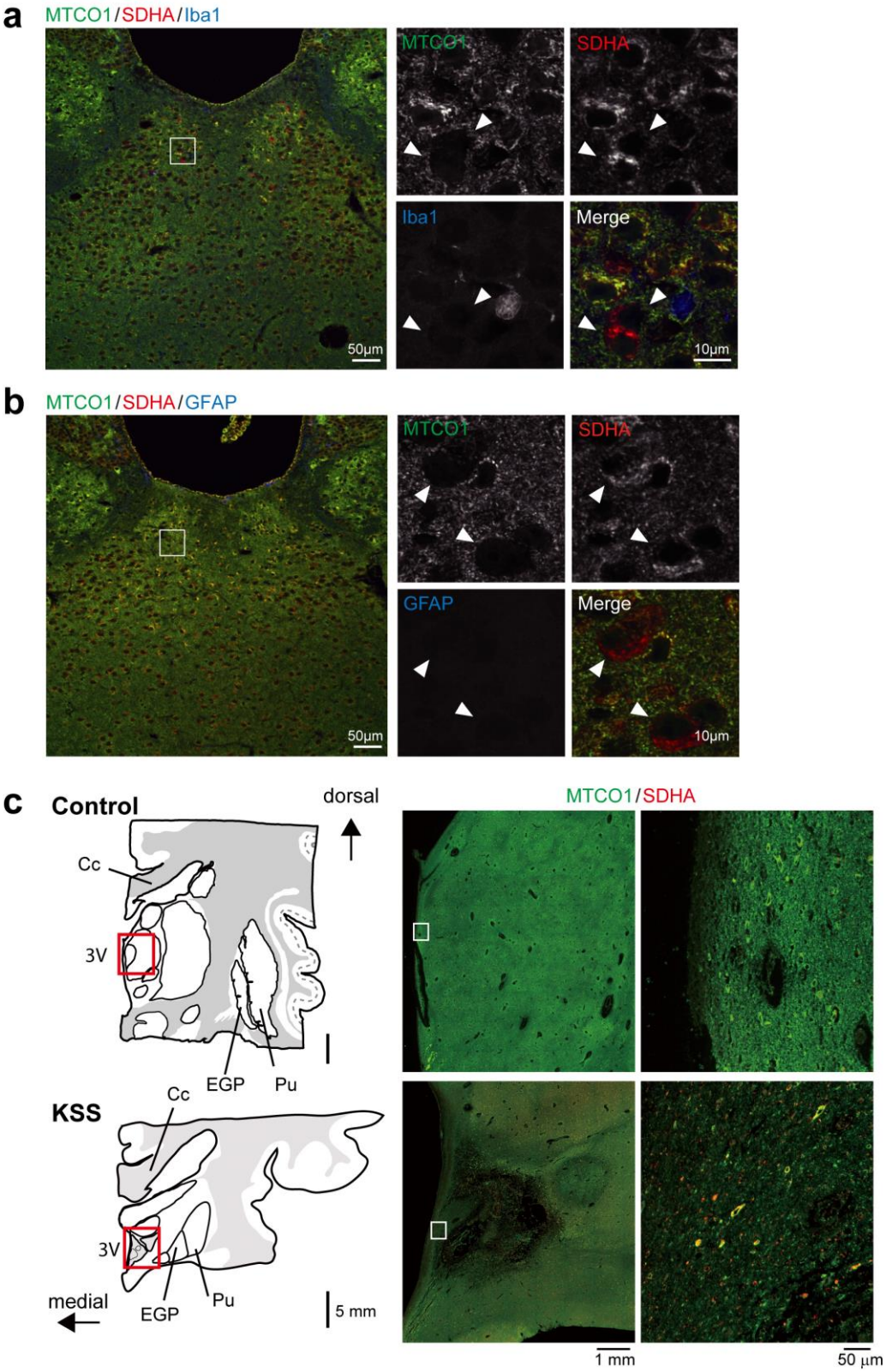

Supplementary Figure 7.

Immunofluorescent staining of COX-negative cells in the PVT region.

(**a**) Triple staining of PVT of *Polg1* mutant mice using anti-MTCO1 (green), anti-SDHA (red),

and anti-Iba1 (blue) antibodies. Higher magnification images of the indicated region (a white rectangle; left) are shown in the right panels. COX-negative cells in the PVT, indicated by arrowheads, are negative for Iba1, a microglial marker.
(**b**) Triple staining of PVT of *Polg1* mutant mice using anti-MTCO1 (green), anti-SDHA (red), and anti-GFAP (blue) antibodies. COX-negative cells in the PVT are negative for GFAP, an astrocyte marker. GFAP-positive cells were hardly observed in the PVT.
(**c**) Double immunofluorescent staining of paraventricular thalamus of a patient with KSS, a severe form of CPEO, and mood symptoms such as euphoria and irritability, and a control subject. The postmortem brain sections (drawings in left panels) were stained using anti-MTCO1 (green) and anti-SDHA (red) antibodies. Medium magnification images of the indicated regions (blue rectangles; left drawings) are shown in the middle panels, and higher magnification images of the indicated regions (white rectangles; middle) are shown in the right panels. Scale bars, 5 mm (left), 1 mm (middle), 50 μm (right). Pu, putamen; EGP, external globus pallidus; Cc, corpus callosum; 3V, third ventricle.

Supplementary Movies 1–3.

Behaviors of a female *Polg1* mutant mouse experiencing depression-like episode in a home-cage with a wheel.

Supplementary Movie 1

Supplementary Movie 2

Supplementary Movie 3

These 10-min movies were videotaped at ZT 18 (2:00–2:10 local time) of the days before (**Supplementary Movie 1**), during (**Supplementary Movie 2**), and after (**Supplementary Movie 3**) depression-like episode. A drinking water faucet and a feedbox are located at the left and right sides of the screen, respectively. The cage was illuminated with infrared LED light all day in order to film the animal even in the dark period.